Currents and Temperatures as Observed in Drake Passage During 1975

R. Dale Pillsbury

School of Oceanography, Oregon State University, Corvallis 97331

Thomas Whitworth III and Worth D. Nowlin, Jr.

Department of Oceanography, Texas A&M University, College Station 77843

Frank Sciremammano, Jr.

School of Oceanography, Oregon State University, Corvallis 97331

(Manuscript received 15 August 1978, in final form 20 November 1978)

ABSTRACT

Current and temperature records from 10 meters on six year-long moorings deployed during February 1975 in Drake Passage are examined and discussed in the context of hydrographic data from that area. The mean flow directions are consistent with those from geopotential anomaly charts, showing a northward flow in the central passage and eastward through-passage flow in the south and north. Directly measured vertical shear below 1000 m is remarkably uniform with depth in the central passage. Periods of high shear correspond to periods of high speed and are associated with lateral shifts in the velocity cores imbedded in the Antarctic Circumpolar Current at Drake Passage. Fluctuations in temperature and current are highly correlated in the vertical. Although meters near 2700 m separated by 80 km or more show only a few significant horizontal correlations for record-length statistics, there appear to be coherent fluctuations in the central passage during winter. Temperature and speed variability suggest that there are distinct thermal and kinematic regimes in Drake Passage.

1. Introduction

During the austral summer of 1974–75 an experiment was begun in Drake Passage to determine the energy-containing space and time scales of the Antarctic Circumpolar Current (ACC), and to describe selected property distributions and phenomena in the region. This first phase of the experiment, called the First Dynamic Response and Kinematics Experiment (FDRAKE), was conducted with three ships and included hydrographic, chemical, meteorological, sea level and current measurements. In this paper we present the temperature and velocity time series data from the moored array as well as interpretations and comparisons with the hydrographic data.

The only previous time series in Drake Passage have been short-term measurements by Reid and Nowlin (1971) and Foster (1972). Reid and Nowlin deployed seven current meters which recorded currents 300 m above the bottom for periods between 25 and 94 h. Foster describes an array of four moorings which recorded current and temperature at 150, 1500 and 3300 m for periods of 4.3 to 10.7 days. The measurements of Reid and Nowlin showed mean currents at all locations to have an eastward component, while all four of Foster's deep meters showed westward flow.

The array of internally recording current and temperature meters described in this paper was deployed by the R/V *Melville* during FDRAKE 75, which began 19 February and ended 30 March 1975. The array was designed to yield information about the space and time scales of variability in Drake Passage. Specifically sought was information regarding the magnitudes, seasonal variability and spatial coherences of currents and temperatures which might be used in designing a long-term experiment to monitor the transport and study the dynamics of the Antarctic Circumpolar Current. Several specific studies using data from this array have been published: Bryden and Pillsbury (1977) analyzed the spatial and temporal variability of the currents at 2700 m; Nowlin *et al.* (1977) used the directly measured currents to reference geostrophic speeds and provide a new short-term estimate of transport through Drake Passage; and Bryden (1979) calculated heat fluxes resulting from low-frequency energetic fluctuations in the current.

0022-3670/79/030469-14$07.50

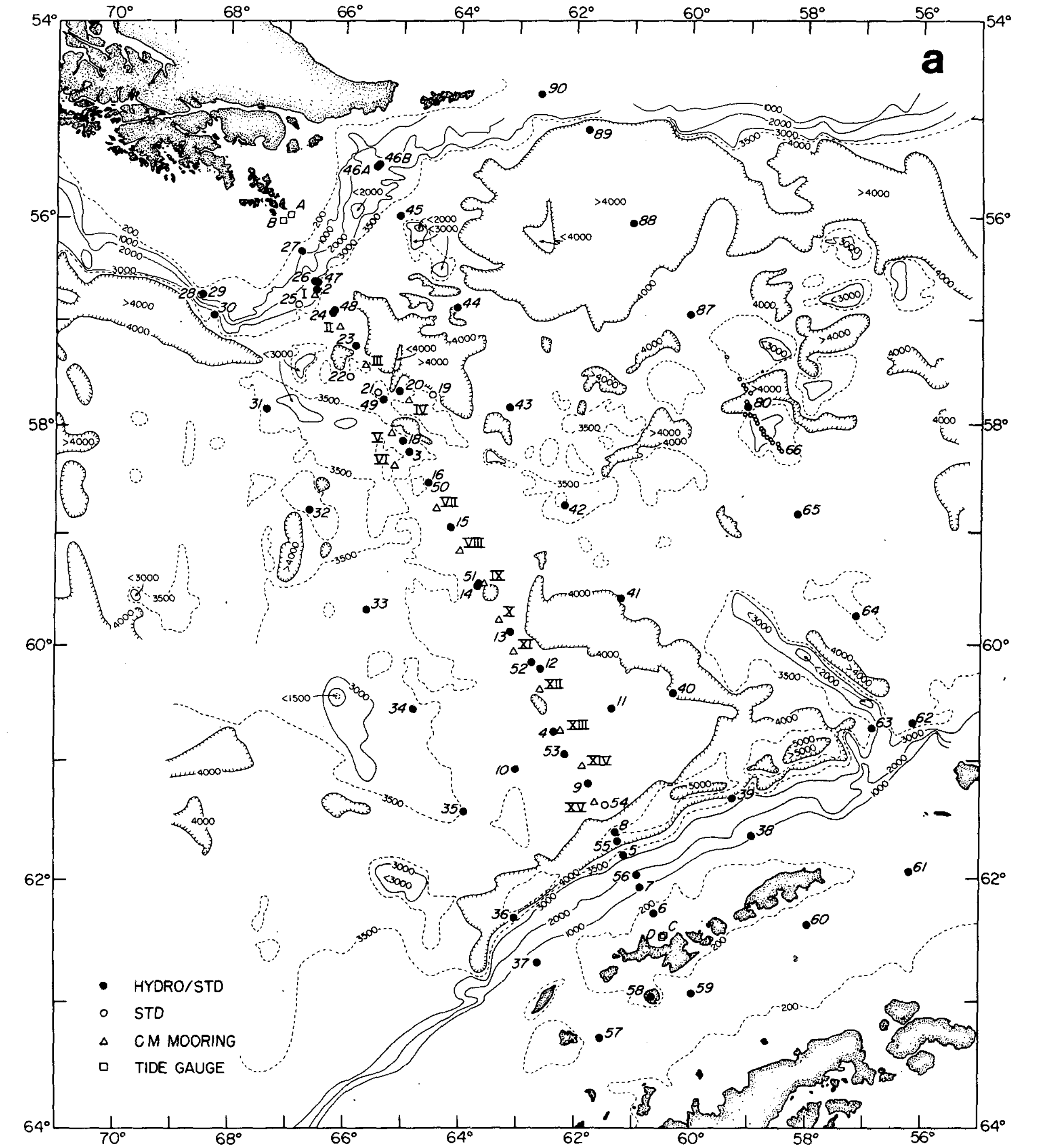

FIG. 1a. Positions of stations and moorings of R/V *Melville* during FDRAKE 75, 19 February–30 March 1975.

2. The data set

In Figs. 1a and 1b are shown the mooring positions and vertical configuration of the array. (Fig. 1a shows the positions of hydrographic stations and moorings while Fig. 1b is an array in vertical section distinguishing long-term from short-term meters.) The array consisted of seven deep moorings in place for a three-week period of the *Melville* cruise and eight deep moorings recovered after one year during the FDRAKE 76 cruise of the *Thompson*. These subsets of the array are called the short-term and long-term arrays, respectively.

The instruments used were Aanderaa RCM5 current meters. The mooring system was designed at Woods Hole Oceanographic Institution (WHOI) for

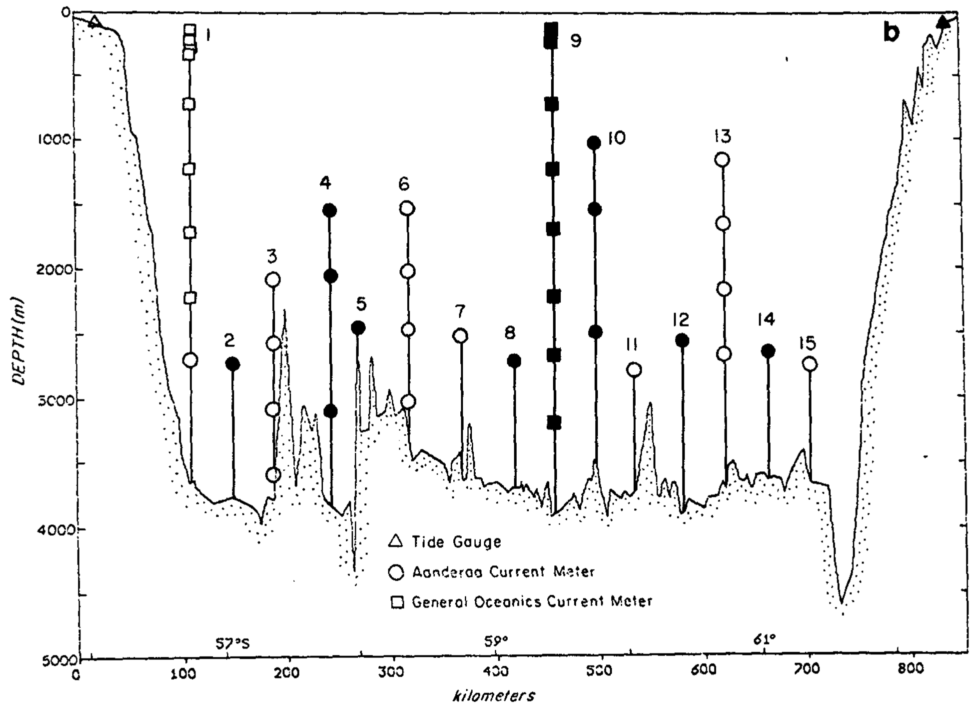

FIG. 1b. Vertical section across Drake Passage showing positions of moored instruments deployed during FDRAKE 75. Solid symbols denote instruments deployed for one year.

intermediate moorings (Heinmiller and Walden, 1973), and has proven very successful in the North Atlantic in moderate currents. To insure that moorings would survive an entire year in an unknown winter environment, few meters were placed near the surface where currents were expected to be strong, and the moorings were deployed with little reserve buoyancy in order that they would yield to high speeds rather than drag their anchors.

Most RCM5's were equipped with special narrow-range thermistor circuits, and high-precision temperature measurements were obtained. These temperature data are a mixture of true temperature variations at fixed points and variations due to vertical excursions of the moorings. While the velocity measurements are also known to be contaminated by this motion, our calculations using numerical models developed at WHOI show a worst case error in speed to be only 9%. During nearly all of the velocity time series, the speed errors due to mooring motions are computed to be less than 3%. Because mooring motion tends to reduce maximum speeds and increase minimum speeds, the error contributed to the mean speed will be smaller than the errors in maxima and minima.

All of the current meters were recovered with the exception of the one on mooring five, and most yielded good data. All current meters were calibrated before and after the experiment; no significant differences were found. The data from the short-term and long-term arrays are presented in Pillsbury *et al.* (1976, 1977).

Although variations with many time scales are ap-

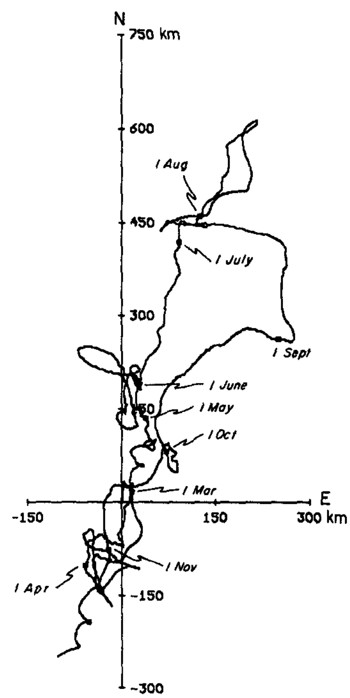

FIG. 2. Progressive vector diagram of the current record from 2771 m at mooring 2 (291-day record).

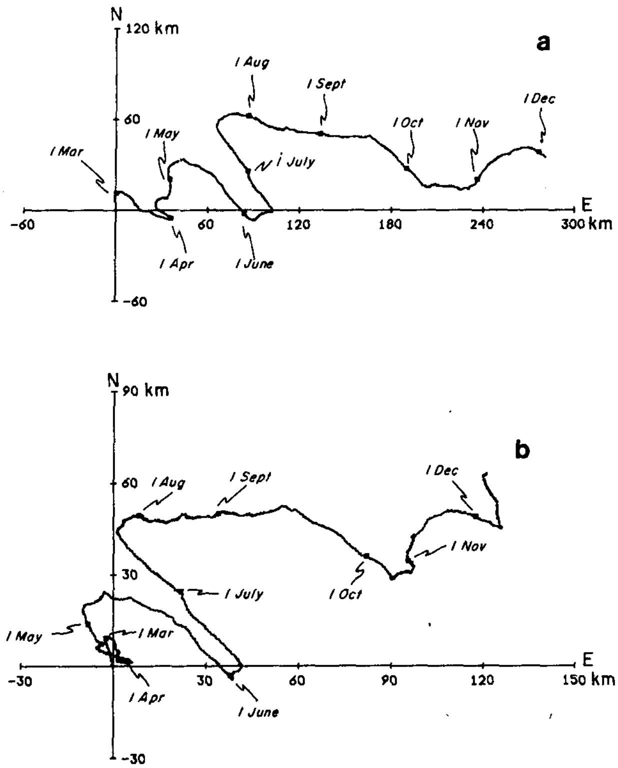

FIG. 3. Artificial progressive vector diagram for mooring 4 at (a) 1337 m (283-day record) and (b) 1837 m (308-day record). Recorded direction and constant speed (3 cm s^{-1}) were used.

parent in the records, the discussion in this paper is limited to lower frequency variations. The hourly data have been filtered using a filter with a half-power point of 40 h which effectively removes the energetic semidiurnal, diurnal and inertial oscillations from the records. Since the records from the short-term array are too short to use in investigating the lower frequencies, only data from the long-term array are considered in this paper.

The progressive vector diagrams (PVD's) of the current records from moorings 2, 4, 8, 10, 12 and 14 are shown in Figs. 2–7. PVD's for the relatively short records from mooring 9 are not included. The two top current meters on mooring 4 gave no speed data, although the records for direction are good. Artificial PVD's (Fig. 3a and 3b) were constructed using these direction data and a constant speed of 3 cm s^{-1}. They are useful in visualizing the direction of flow and the vertical coherence at this mooring.

In Fig. 8 are the daily mean stick figures from the deep meters (near 2700 m) on the long-term moorings 2, 4, 8, 10, 12 and 14. Also shown in Fig. 8 are plots of temperature versus time plotted every 6 h for each of the deep meters. The daily mean current vectors from the three meters on mooring 10 are shown in Fig. 9. The stick figures are not presented in a true north-south, east-west coordinate system, but rotated to conform to through-passage (positive toward 62° True) and cross-passage (positive toward 152° T) directions.

Table 1 gives selected statistical information for the low-passed records of current and temperature. At mooring 2 in the northern passage high speeds occur even at depth. The maximum speed recorded was 50 cm s^{-1}, and during several periods of the year speeds in excess of 30 cm s^{-1} were common. These relatively large speeds were accompanied by considerable variability in direction, however, resulting in very little net flow over the entire record length (see Fig. 2). The net flow components for the record length were 0.41 cm s^{-1} to the west and 0.99 cm s^{-1} to the south. It should be noted that this record may not be representative of the mean flow through the passage at this location because the meter was located just above the region of rough bottom topography in the northern passage. Nowlin *et al.* (1977) show that the pattern of vertical coherence in the property distributions at the level of

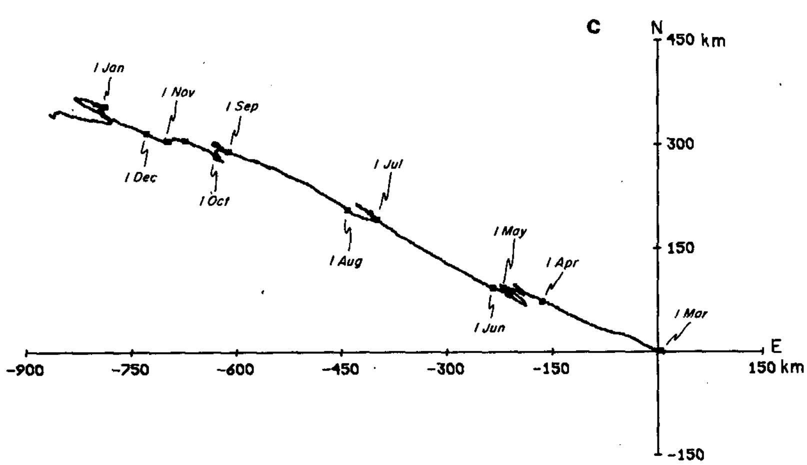

FIG. 3c. Progressive vector diagram of the current record from 2837 m on mooring 4 (342-day record).

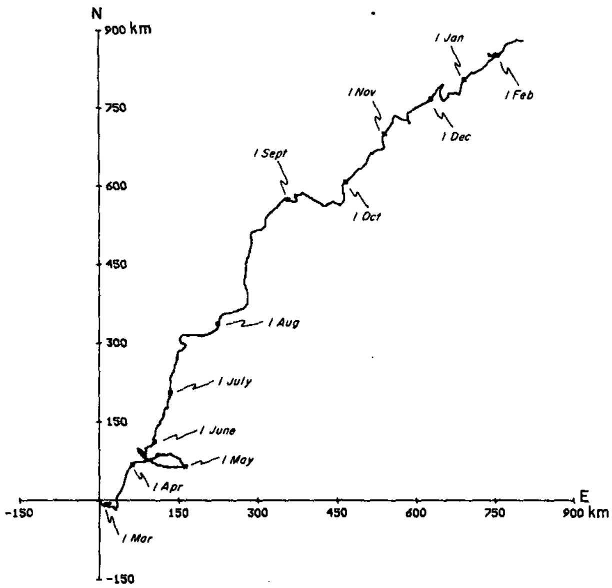

FIG. 4. Progressive vector diagram of the current record from 2741 m on mooring 8 (351-day record).

the current meter is disrupted, probably by topographic effects.

At mooring 4, the flow at the upper meters (Fig. 3a and 3b) was generally eastward. The meter at 2840 m on mooring 4 (Fig. 3c) gave a record unlike those from other meters in the passage. The meter was situated in a channel and the flow direction was bimodal, confined to up and down channel.

The maximum speed recorded at mooring 8 was 27 cm s^{-1} while the mean was 7.1 cm s^{-1}. The means for the north and east components of velocity were 2.9 and 2.7 cm s^{-1}, giving a resultant mean flow to the northeast. This record shows a significantly greater net flow than observed at mooring 2.

Eighty kilometers south of mooring 8, at mooring 10, the mean current was almost due north having northward and eastward velocity components of 5.9 and −0.3 cm s^{-1}. The mean current at mooring 10 showed a clockwise rotation with increasing depth. At the upper meter (1019 m) the northward and eastward mean components were 8.6 and 3.4 cm s^{-1}.

At mooring 12 the mean speed was 6.6 cm s^{-1}, which is a little less than the 7.4 cm s^{-1} mean from the deep meter on mooring 10. The north component at mooring 12 was 4.4 cm s^{-1}, while the west component was 1.5 cm s^{-1}, indicating mean flow to the northwest.

The mean deep flow (2667 m) at mooring 14 was almost directly to the east. The east component at

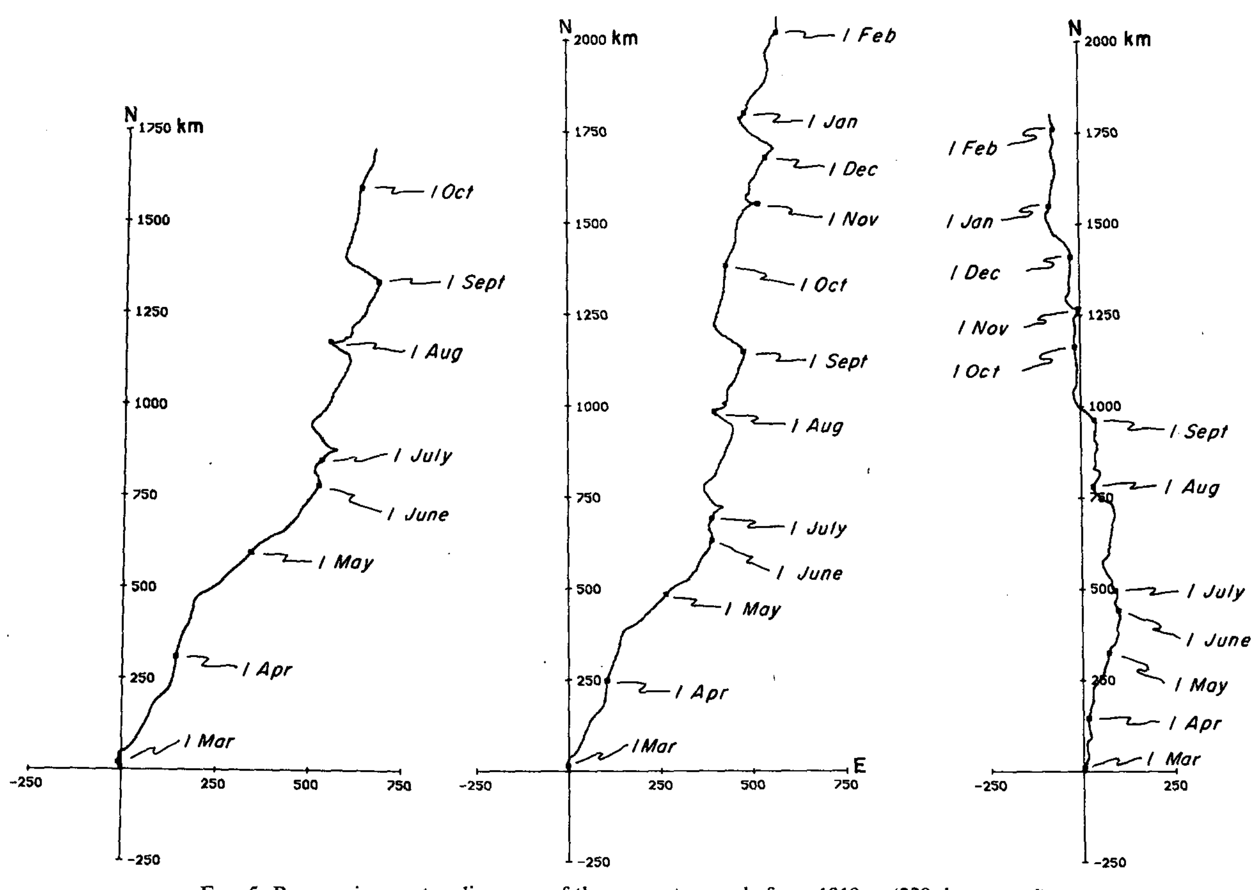

FIG. 5. Progressive vector diagrams of the current records from 1019 m (229-day record), 1519 m and 2519 m (352-day records) on mooring 10.

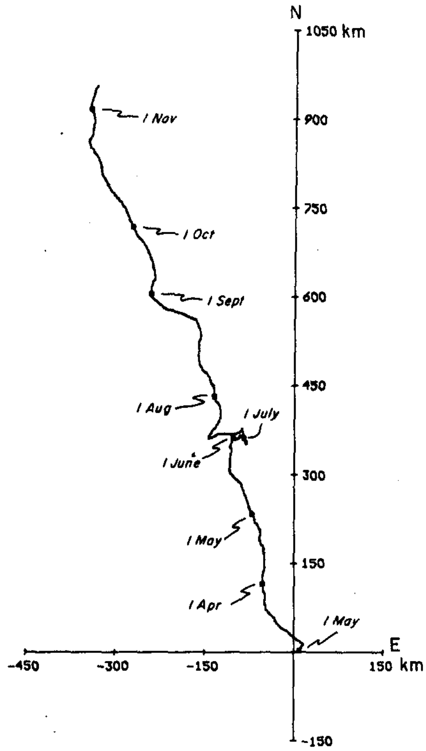

FIG. 6. Progressive vector diagram of the current record from 2604 m on mooring 12 (254-day record).

this meter was 5.5 cm s^{-1}, while the north component was only 0.4 cm s^{-1}.

3. Observed variations in the context of the regional hydrography

To aid interpretation of the time series, two representations of the regional hydrography are shown. Fig. 10 (adapted from Nowlin *et al.*, 1977) shows the temperature distribution during the first week in March 1975 (immediately after current meter deployment). The evident bands of large horizontal temperature gradient are associated with transitions between distinct water mass regimes. As discussed by Nowlin *et al.* (1977), these transition zones are bands of relatively large horizontal density gradients and, therefore, of large eastward geostrophic shear relative to depth. The positions of these current bands relative to the long-term moorings shortly after deployment can be seen in Fig. 10.

Fig. 11 shows the geopotential anomaly of the 2500 db surface relative to 3250 db as constructed from hydrographic data collected during March of 1975 at the indicated station locations. Also shown are the record-length mean velocities at the deep current meters. This pattern of geopotential anomaly in the deep layers is similar to representations from historical data of geopotential anomaly (Reid and Nowlin, 1971) and the topography of density surfaces (Gordon, 1967; Gordon and Molinelli, 1975). The horizontal distribution of temperature at 2700 m during March 1975 (not shown) resembles both the pattern shown in Fig. 11 and that from historical data between 2000 and 3000 m (Gordon and Goldberg, 1970). We will consider the pattern of Fig. 11 to be representative of the flow direction near the deep meters.

Although the general through-passage direction is ~62°T (which is the direction of the ordinate of the sticks in Fig. 8 and 9) the flow in the northern and central passage is toward the north and even west-northwest in some locations. The historical data suggest that this pattern may be a permanent feature in Drake Passage.

In the central passage (moorings 8, 10 and 12) the direction of mean flow rotates from northeastward at mooring 8 to north-northwestward at mooring 12. The turning is consistent with the direction of geostrophic flow (Fig. 11) and is in response to the ridge extending northwest from Elephant Island. Mooring 14 lies west and south of the northward turning of the flow and shows net eastward flow.

Temperature data from these moorings show a combination of two signals. One of these is due to advection of water of varying temperature past the instrument; the other is due to the vertical motion of the instrument in a vertically stratified temperature field. Based on the hydrographic measurements the vertical temperature gradients were about 1°C (1500 m)$^{-1}$ at the locations of most instruments. The corresponding horizontal gradients were about 1°C (300 km)$^{-1}$. We estimate that while the vertical motions can be as much as 150 m for the top meters on

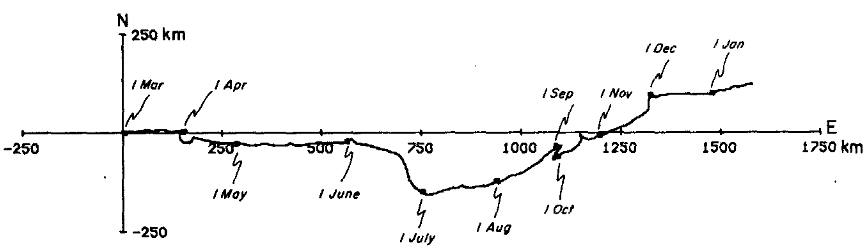

FIG. 7. Progressive vector diagram of the current record from 2667 m on mooring 14 (332-day record).

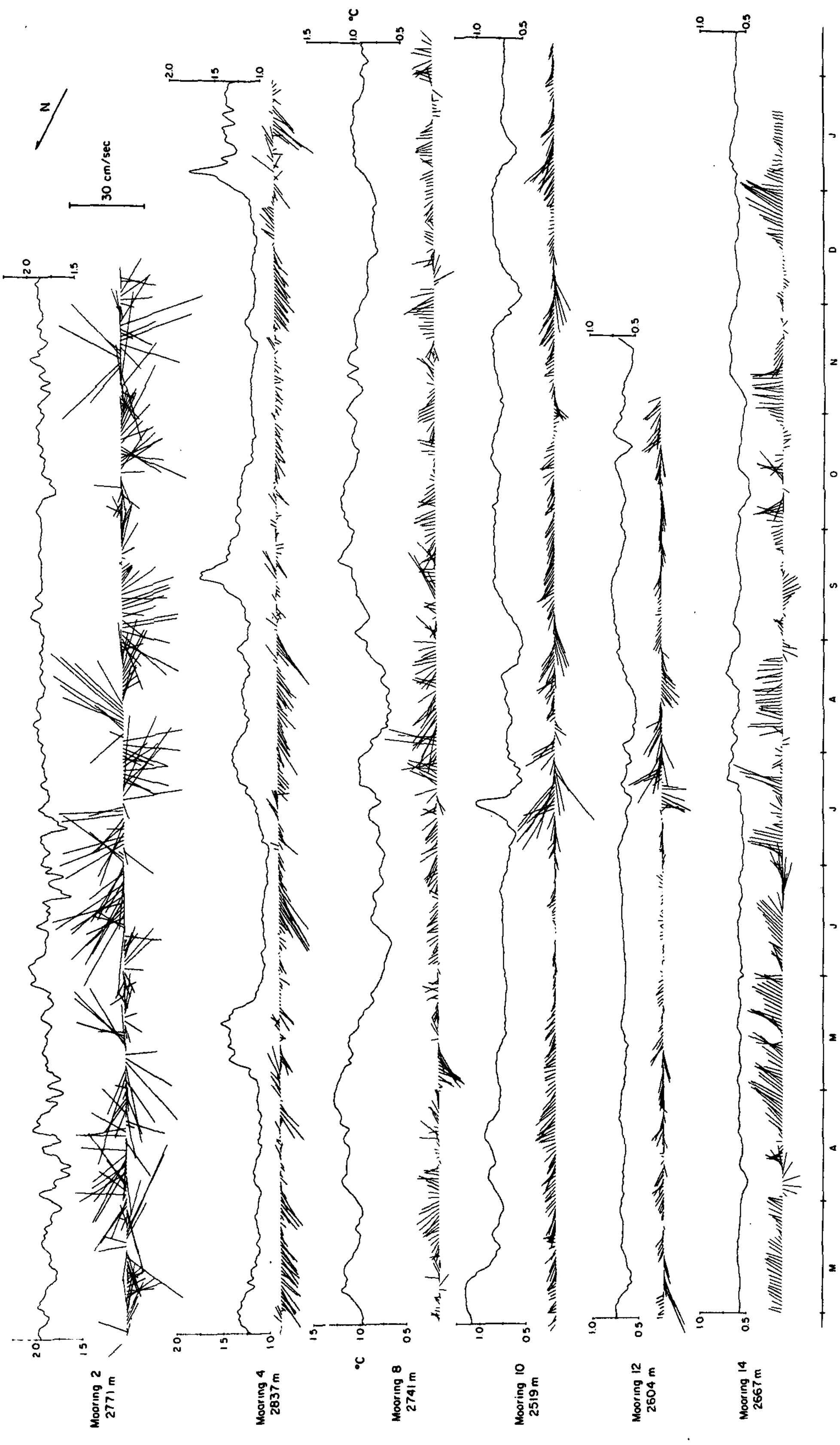

FIG. 8. Daily mean current vectors and temperatures from the deep meters on moorings 2, 4, 8, 10, 12 and 14.

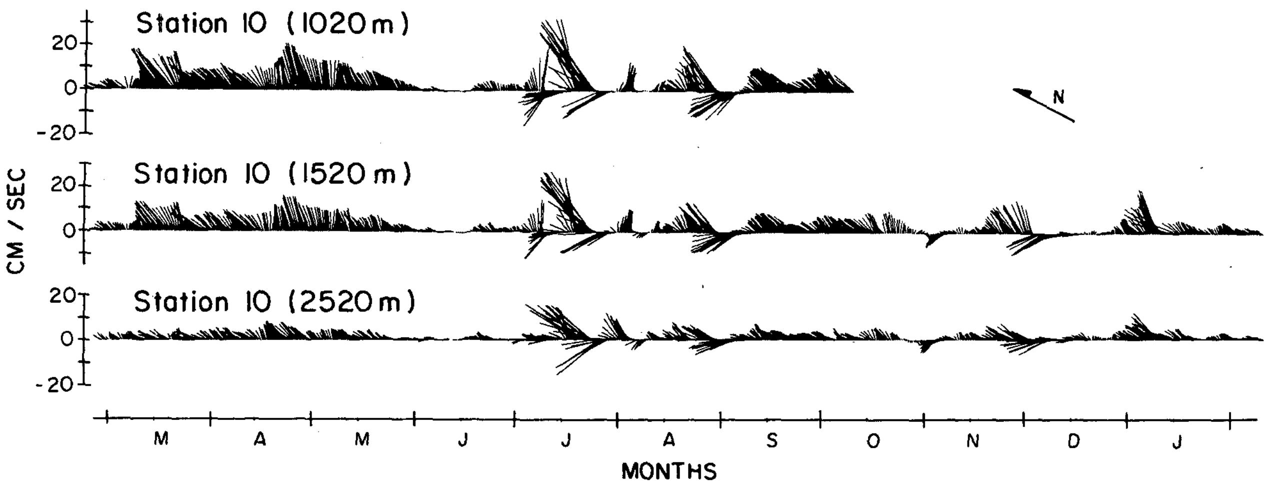

FIG. 9. Daily mean current vectors from the three current meters on mooring 10.

moorings 4 and 10, the excursion is typically less than 50 m for the deeper meters. The maximum contribution to the signal from vertical motions is of the order of 1°C $(1500 \text{ m})^{-1} \times 150$ m = 0.1°C for the upper meters and 0.03°C for the deeper ones. The average observed range for the temperature records is 0.7°C, implying that most of the signal must be due to horizontal advection. Since the isotherms at 2700 m generally parallel the isopleths in Fig. 11, it is clear that either east–west or north–south shifts in the flow pattern will result in temperature changes at the mooring sites.

The largest horizontal temperature gradients at 2700 m are in the central passage. Examination of the deep, long records show that temperature excursions were much larger at the mid-passage moorings than at moorings 2 and 14 at the northern and southern sides of the passage. Also notable are the high-frequency temperature oscillations at mooring 2, perhaps associated with the energetic oscillations and flow reversals evidenced in the current record.

Some of the most striking features of the time series are the occurrences of intermittent "events" in both current and temperature. Even the record from the deep meter on mooring 4 which is located in a channel shows several distinct temperature fluctuations. Except for mooring 2, most of the yearlong temperature variability is due to the events which are especially strong during the winter at mid-passage moorings.

The events are likely related to aperiodic translations of the high-speed cores and their associated large horizontal temperature gradients, or to the passage of eddies (Joyce and Patterson, 1977). Either of these mechanisms could produce velocity and temperature perturbations at a particular current meter, but the effect on adjacent moorings would depend on the horizontal scale of the event-causing mechanism.

TABLE 1. Selected record-length statistics from 1975 array in Drake Passage.

Mooring no.	Depth (m)	Duration (days)	$\bar{u}$* (cm s^{-1})	Standard deviation u (cm s^{-1})	$\bar{v}$* (cm s^{-1})	Standard deviation v (cm s^{-1})	Mean speed (cm s^{-1})	$\bar{T}$ (°C)	Standard deviation T (°C)	T_{max} (°C)	T_{min} (°C)
2	2770	291	−0.4	12.4	−1.0	14.4	16.6	1.87	0.07	2.06	1.51
4	1340	305	—	—	—	—	—	2.13	0.12	2.39	1.78
4	1840	324	—	—	—	—	—	1.80	0.14	2.16	1.41
4	2840	342	−2.9	6.3	1.2	4.4	6.8	1.21	0.14	1.86	0.97
8	2740	351	2.7	5.2	2.9	5.0	7.1	0.95	0.15	1.33	0.60
9	1200	149	3.6	7.1	1.7	6.0	8.9	—	—	—	—
9	1700	68	4.9	5.6	4.4	5.0	9.0	—	—	—	—
10	1019	275	3.4	7.7	8.6	6.9	11.3	1.81	0.16	2.19	1.20
10	1519	352	1.9	6.6	6.8	5.8	9.7	1.42	0.16	1.93	0.91
10	2519	352	−0.3	4.5	5.9	4.6	7.4	0.77	0.12	1.19	0.47
12	2600	253	−1.5	4.6	4.4	4.6	6.6	0.65	0.06	0.79	0.47
14	2670	331	5.5	6.0	0.4	4.2	7.8	0.59	0.05	0.75	0.46

* u is the eastward component and v the northward component of speed.

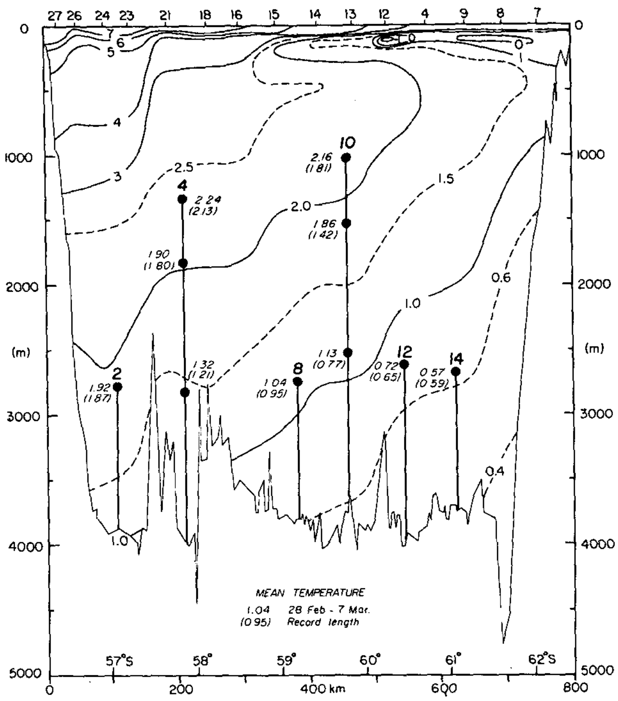

FIG. 10. Temperature across Drake Passage from station data collected during the first week in March 1975 (after Nowlin *et al.*, 1977). Also shown are mean temperatures for that week and for the entire record length (in parentheses) as recorded by the long-term meters.

4. Vertical shear

Information about the vertical structure of the horizontal current can be found in the data from mooring 10. Here three meters in the vertical (1019, 1519 and 2519 m) gave good speed, direction and temperature data for more than eight months. The two deeper meters ran for the entire installation period of one year.

In order to compare the directly measured shear to the shears from hydrographic stations, some averaging period for the current meter measurements must be selected. Autocorrelation functions were constructed for the vertical shears of the through-passage and cross-passage current between 1019 and 1519 m and between 1519 and 2519 m at mooring 10. From these, the time scales of independence for the shears of through-passage and cross-passage flow were estimated to be 7.5 and 16 days, as defined by the average values of the first zero crossing of the autocorrelation function.

Fig. 12a shows the through-passage shear values for the records after a filter with a half-power point of 7.5 days was applied. The shear is uniform with depth to a remarkable degree. The variability in the shear is higher during winter when several changes between maximum and minimum shear occur within short periods (1 week). In fall, there is a slower transition from maximum shear to a more barotropic condition. The agreement between the shears (upper minus mid-depth, mid-depth minus lower) is better during the rapid changes in winter. The good agreement and rapid changes in shear further suggest that the winter events may be associated with advective processes.

Fig. 12b shows the cross-passage shear values at mooring 10 after application of a filter with a half-power point of 16 days. After smoothing with this filter the cross-passage shears are also quite uniform with depth.

Nowlin *et al.* (1977) have shown that shears of through-passage currents from direct measurements at these moorings agree well with geostrophic shears from stations spanning the moorings provided the measured currents are averaged over at least several days. As shown in Fig. 13a, the average through-passage shear between the upper-middle and middle-lower current meters on mooring 10 is between 2×10^{-3} and 3×10^{-3} cm s^{-1} m^{-1}. The average shear from all hydrographic stations made at the time of installation and time of recovery of the array was 2×10^{-3} cm s^{-1} m^{-1} between 1000 and 1500 m and 1.5×10^{-3} between 1500 and 2500 m [values from Nowlin *et al.* (1977, Fig. 10)]. A second shear estimate was made using only those hydrographic stations which spanned current cores. Values ranged from 7 to 18×10^{-3} cm s^{-1} m^{-1}, as compared to

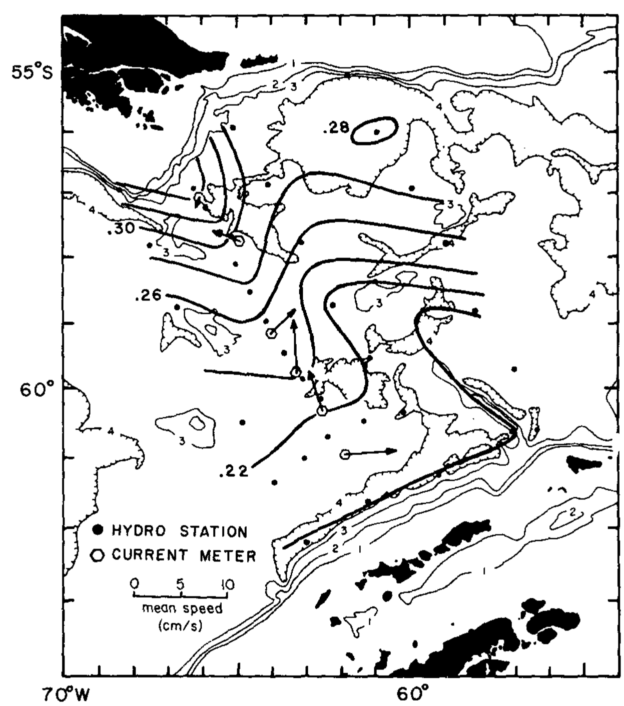

FIG. 11. Dynamic topography (dynamic meters) of the 2500 db surface relative to 3250 db from hydrographic measurements (at indicated positions) made during March 1975. Vectors show the record-length mean velocities recorded by the deep current meters near 2700 m.

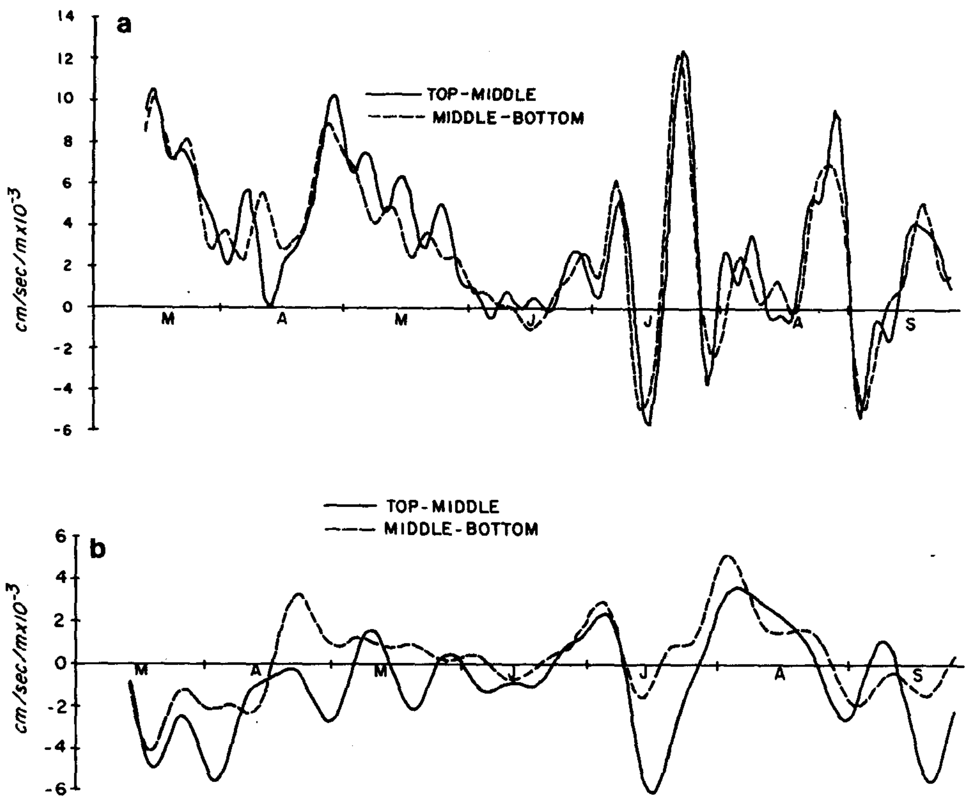

FIG. 12. Time series of (a) through-passage shear (7.5-day filtered) and (b) cross-passage shear (16-day filtered) between the current meters on mooring 10.

peak values of at least 10×10^{-3} cm s^{-1} m^{-1} which were approached four times during the seven-month record from mooring 10 (Fig. 12a). These consistent values suggest that mooring 10 was in or near a high-speed core at least four times during the year.

Since the direction of flow associated with the current core varies, we have calculated the magnitude of the shear between the upper and middle and the middle and lower meters at mooring 10 (Fig. 13). This shows evidence for the passage of several cores past the mooring. The four cases noted in Fig. 12a are also seen in this figure, but it appears that there may have been additional core passages.

In view of the banded nature of the density field as evidenced by hydrographic data taken across the passage in 1975, 1976 and 1977, it is reasonable to assume that when the shear is large the currents at the upper meters will be large, and when the shear is small the currents throughout the water column will be small. At the upper meter at mooring 10 (1019 m) the mean speed was 11.3 cm s^{-1} with a standard deviation of 7.1 cm s^{-1}. The speed at the upper meter rises at least one standard deviation above the mean (18.4 cm s^{-1}) six times during the length of the shear record. These times are indicated by arrows in Fig. 13. Clearly, speed maxima occur at peaks in the vertical shear of speed.

5. Cross correlations from time series measurements

a. *Vertical correlations*

The vertical coherence over the long-term current records is high as evidenced by Figs. 3a and 3b for mooring 4 and Figs. 5 and 9 for mooring 10. The time series of low-passed temperatures plotted every 6 h for these moorings (Fig. 14) also show high vertical coherence.

In Table 2 we present estimates and confidence limits of vertical cross-correlation coefficients of temperature, velocity components and fluctuation kinetic energy at moorings 4 and 10. Confidence limits are expressed in terms of the large-lag standard error σ calculated from the Bartlett formula. The unknown distribution function of the correlation estimates determines the significance level. The 3σ level would represent the 90% confidence level for a random distribution or the 99% confidence level for a normal distribution. Because the record lengths for each current meter are different, Table 2 presents a normalized quantity (cross-correlation coefficient divided by 3σ) to permit a direct comparison of the correlations between different levels.

An examination of the coherence plots (not shown) indicates that the major contribution to the correlation is made at low frequencies. Bryden

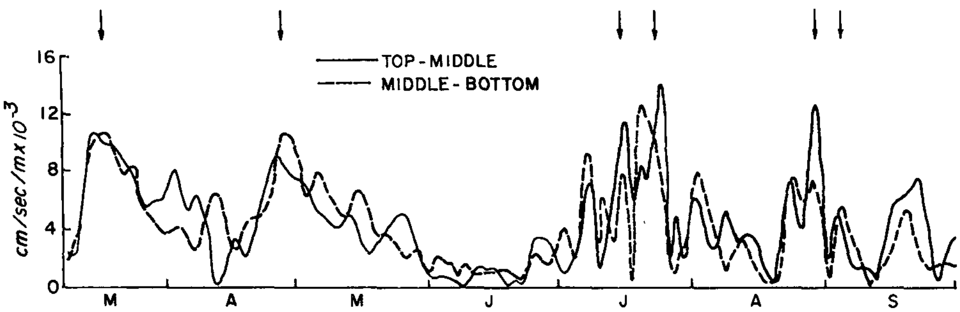

FIG. 13. Magnitude of the shears between the upper and middle and the middle and lower meters at mooring 10. Arrows show times at which the speed at the upper meter is more than one standard deviation above its mean speed.

(1979) has examined low-frequency fluctuations from mooring 10 in the band 0.058–0.068 cycles day^{-1} (cpd) which has high values of squared coherence. He found that temperature fluctuations were in phase at all depths, while velocity fluctuations at 2519 m lead those at 1019 m by about 35°. His findings are confirmed by our cross-correlation calculations which include fluctuations at all frequencies. At mooring 10 the velocity fluctuations occur first at the lower meter and appear to propagate upward at a consistent rate (within the error estimates of the lags, which is ~6 h). Fluctuation kinetic energy and temperature oscillations seem to occur at all depths simultaneously. At mooring 4 the correlations of temperature between the bottom meter and the other meters are not as high as the temperature correlation between the upper two meters. Moreover, temperature variations at the lower meters are seen to lag considerably those at the upper meters.

At mooring 4 the time variations of the current direction are similar at the upper two meters as suggested by the pseudo PVD's (Fig. 3). Several periods of southwest–northeast flow are seen to occur at approximately the same time. Similar flow reversals occur at the lower meter as well although it was

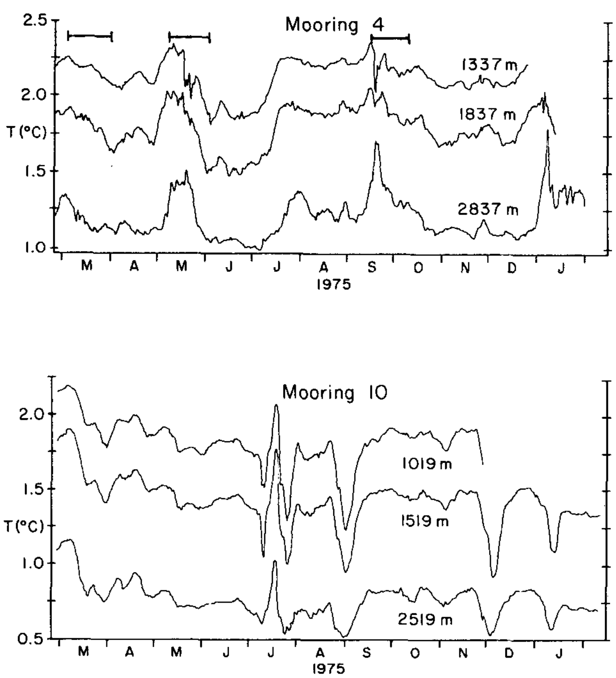

FIG. 14. Time series of low-passed temperature from the three current meters on moorings 4 and 10. Bars indicate periods of southeastward flow at mooring 4 (see text).

TABLE 2. Estimates and confidence limits of vertical cross-correlation coefficients at moorings 4 and 10.

	Cross-correlation coefficient	3σ*	Cross-correlation coefficient $\div 3\sigma$	Lag** (h)
Mooring 10				
1019–1519 m				
$T \times T$	0.96	0.67	1.43	0
$u \times u$	0.98	0.45	2.18	6
$v \times v$	0.96	0.57	1.68	6
KE′ × KE′	0.96	0.52	1.85	6
1519–2519 m				
$T \times T$	1.00	0.56	1.79	0
$u \times u$	0.83	0.35	2.37	12
$v \times v$	0.85	0.42	2.02	12
KE′ × KE′	0.84	0.39	2.15	0
1019–2519 m				
$T \times T$	0.92	0.65	1.42	0
$u \times u$	0.75	0.40	1.88	18
$v \times v$	0.73	0.53	1.38	18
KE′ × KE′	0.78	0.49	1.59	0
Mooring 4				
1337–1837 m				
$T \times T$	0.90	0.84	1.07	6
1837–2837 m				
$T \times T$	0.78	0.69	1.13	108
1337–2837 m				
$T \times T$	0.74	0.75	0.99	126

* The large-lag standard error σ was calculated using the Bartlett formula. For a Gaussian distribution of the correlation function, 3σ represents the 99% confidence level. For a random distribution using Chebychev's inequality, 3σ represents the 90% confidence level.

** The lower meter leads the upper.

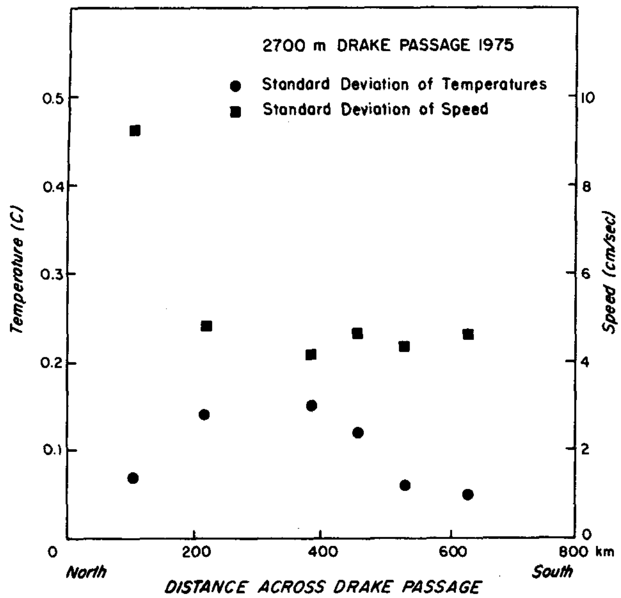

FIG. 15. Standard deviations of temperature and speed for the six long-term meters near 2700 m.

located in or just above a channel which constrained the flow to be bi-directional. The upper two meters on mooring 4 produced the only records in which direction and temperature have a consistent relationship. During each period of southeastward flow (indicated by bars on Fig. 14) the temperature decreased.

b. *Horizontal correlations*

The 1975 moorings were separated by horizontal increments of ~80 km. We have examined these records for cross-correlation and coherence at separations in the cross-passage direction from 80 km to over 500 km. Based on the record-length analysis for this range of separations the cross-correlation coefficients for temperature, through-passage and cross-passage speed and fluctuation kinetic energy were generally below the 3σ confidence level. The kinematic quantities $v \times v$, $u \times u$ and $KE' \times KE'$ gave cross-correlation coefficients near or above 3σ for some pairs of moorings at the shortest separations. These cases are discussed below. The 1976 and 1977 records from the Drake Passage can be used to examine coherence and correlation for smaller separations (down to 11 km), for which the cross-correlation coefficients in all variables are larger (Sciremammano *et al.*, 1978).

There seem to be distinct kinematic and thermal regimes within Drake Passage based on the cross correlations of velocity components and temperature. The largest cross correlations for speed components are between records taken from moorings 8, 10 and 12 in the central passage. For those pairs the $KE' \times KE'$ cross-correlation coefficients are near or above the 3σ level and the $v \times v$ coefficients are above the 2σ level. Mooring pair 10 and 12 also has a $u \times u$ cross-correlation coefficient larger than 3σ. Moreover, for these three central passage moorings the coherence calculations evidence peaks at common periods near 5.5, 3.6, 2.2 and 1.8 days. Most of the fluctuation energy at these moorings as well as the high coherence between them are for periods greater than 33 days. Based on visual inspection of the current records for moorings 8, 10 and 12 (Fig. 8) as well as preliminary analysis for cross correlations using shorter record-lengths, there are high correlations between the velocity fields during the months of July and August. These winter events which are highly correlated in the central passage are probably responsible for the marginally significant correlations in kinematic quantities based on the year-long records.

The cross correlations for $T \times T$ for the longest common data sets are not significant for any pairs of moorings. There are, however, periods of up to a month or longer when there is significant correlation among two or more of the records. The general winter decrease in temperature observed at moorings 8, 10 and 12 during the months of July and August is correlated at a significant level. Moreover, the temperature cross correlations from the year-long records give support for three distinct regions in the passage. The signs of the coefficients are positive for moorings in the central passage (8, 10 and 12) and for moorings at the north and south (2 and 14) but are negative for either 2 or 14 combined with the central moorings.

Omitting calculations involving mooring 4, all other deep meters from 1975 show positive cross

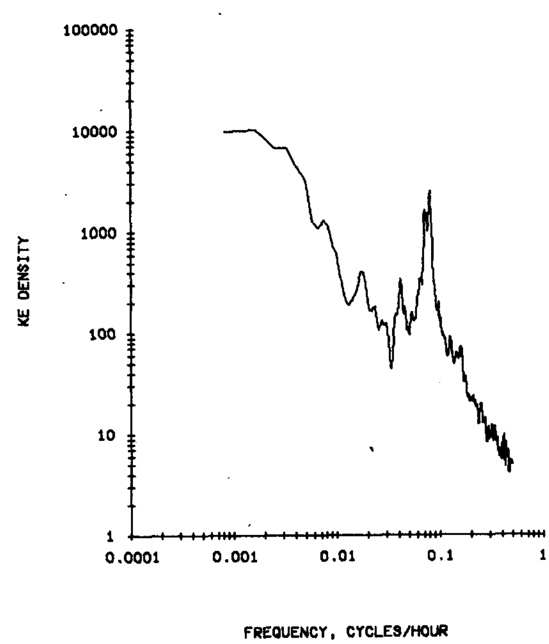

FIG. 16. Current spectrum of the unfiltered data from 2519 m on mooring 10.

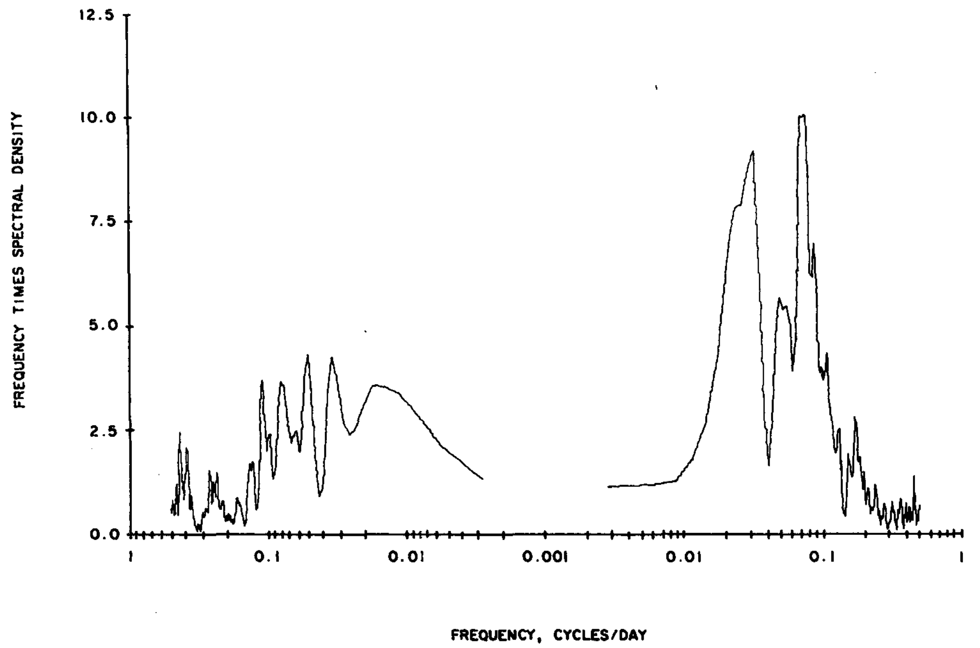

FIG. 17. Rotary spectrum of the low-low passed data from 2519 m on mooring 10.

correlations for fluctuation kinetic energy at the lags of maximum values. This implies that the scale of the energy fluctuations is at least comparable to the size of the passage. On the other hand, the correlation coefficients for KE′ × KE′ vary greatly but not uniformly with separation, implying that scales shorter than distances across the passage are also important.

The cross-correlation coefficients give evidence that the central region differs in several ways from the northern and southern regions. In addition to the higher correlation of motions at moorings in the central passage, the temperatures at these moorings seem to increase or decrease together and in the opposite sense from those in the northern or southern passage.

Differences between these regions can also be seen from the standard deviations of speed and temperature for the six long, deep records across the passage (Fig. 15). These give a measure of the spatial distribution of variability. As expected from inspection of the individual records, the standard deviation of temperatures from the means is significantly larger in mid-passage than at the southern and northern sides. The difference reaches a factor of 3 when comparing mooring 8 with moorings 2 or 14. This can probably be attributed to the meandering of the current regime in mid-passage which causes relatively large horizontal temperature gradients to be advected past those moorings.

In contrast to the temperature records, the standard deviations of speed from the long-term means seem rather uniform at all moorings except the northernmost. For this mooring the speed and standard deviation are larger by a factor of 2 than those of the other deep meters. It may be interactions between the flow and the topography in this region which produce energetic oscillations.

6. Spectral characteristics of time series measurements

A current spectrum (Fig. 16) was calculated from the unfiltered data taken at 2519 m at mooring 10. It is representative of all of the spectra from the current meter array except for mooring 2, which has an order of magnitude more energy in the spectral band from 10 to 100 days. All of the spectra show strong peaks at tidal frequencies. The predominance of tidal and inertial energy in the frequency range of a few hours to a day is not unexpected. There is also considerable energy at 14-day periods which may be related to tidal forcing.

Since there is a strong semiannual period in the winds and atmospheric pressure (Schwerdtfeger, 1962; van Loon, 1967) and an annual period in the thermohaline process, one expects to find energy at those periods in the current and temperature spectra. The increase in kinetic energy toward the low frequencies shown in Fig. 16 indicates that low-frequency variability is present in the data. Fitting a wave of semiannual period to the current meter data shows significant amplitude at all locations (Baker *et al.*, 1977).

The rotary spectrum (Fig. 17) calculated from the filtered data taken at 2519 m on mooring 10 shows more clearly than Fig. 16 the energetic peaks in the mid-frequency range. One sees significant energy in the frequency range of 0.02 cpd (50 days) to 0.18 cpd (5.5 days). Spectra from other long-term moorings show a similar distribution of energy. Significant peaks occur in this record at 0.035 cpd (28 days), 0.054 cpd (18.5 days), 0.075 cpd and 0.18 cpd (5.5 days). The sources of these energetic motions is not well understood, but through-passage geostrophic winds calculated from surface pressure charts show spectral peaks near 5.5 days (Baker *et al.*, 1977) which are related to the observed currents at 1019 at mooring 10, albeit in a mysterious fashion.

7. Summary and conclusions

Current and temperature records from ten instruments moored across the Drake Passage during 1975 were analyzed to determine the important spatial and temporal scales. These records were examined in the context of hydrographic information from that area.

From the two moorings with three instruments in the vertical, the current and temperature variations are seen to be almost perfectly correlated in the vertical for depths >1000 m. The small lag seen in kinematic variables shows the lower meters leading the upper ones.

Below 1000 m the measured vertical shears are quite uniform. Large shear values coincide with high speeds in the upper waters and occur as discrete events in the records. This is consistent with the concept of current cores with large horizontal density gradients separating discrete water masses with smaller horizontal density gradients. The measured values of speeds and shears at the cores agree well with geostrophic calculations made using hydrographic station data.

The mean flow directions at the mooring locations agree in general with the flow field inferred from the contours of geopotential anomaly. The dynamic anomaly patterns relative to deeper layers show eastward through-passage flow in the northern and southern passage, and a northeastward flow in the central passage. The flow at all except deep meters on moorings 2 and 4 seem to fit this pattern. The deep meter on 4 was deployed in a canyon-like feature and the flow was constrained to be bi-directional. In the case of mooring 2 the meter was located not far above major bottom features and probably subject to bathymetric influence.

Based on the record-length analysis, there is little coherence between meters separated by 80 km or more in the cross-passage direction. The cross-correlation coefficients are larger for some selected shorter record lengths. This is particularly true in the central passage during winter, which seems to be dominated by events of scale of several hundred kilometers.

There is evidence that there are distinct thermal and kinematic regimes in Drake Passage. The central passage moorings evidence higher horizontal correlations, greater temperature variability and smaller speed variability than moorings at the northern and southern ends of the passage.

Year-long current and temperature records were also obtained during 1976 and 1977 from arrays in Drake Passage. Data from these arrays are presently under analysis and are expected to yield more complete information about specific processes and regimes in Drake Passage.

REFERENCES

Baker, D. J., Jr., W. D. Nowlin, Jr., R. D. Pillsbury and H. L. Bryden, 1977: Antarctic circumpolar current: Space and time fluctuations in the Drake Passage. *Nature*, **268**, 696–699.

Bryden, H. L., 1979: Poleward heat flux and conversion of available potential energy in Drake Passage. *J. Mar. Res.* (in press).

——, and R. D. Pillsbury, 1977: Variability of deep flow in the Drake Passage from yearlong current measurements. *J. Phys. Oceanogr.*, **7**, 803–810.

Foster, L. A., 1972: Current measurements in the Drake Passage. M.S. thesis, Dalhousie University, 61 pp.

Gordon, A. L., 1967: Structure of Antarctic waters between 20°W and 170°W. *Antarct. Map Folio Ser.*, No. 6, V. Bushnell, Ed., Amer. Geogr. Soc., 10 pp.

——, and R. D. Goldberg, 1970: Circumpolar characteristics of Antarctic waters. *Antarct. Map Folio Ser.*, No. 13, V. Bushnell, Ed., Amer. Geogr. Soc., 1–5.

——, and E. Molinelli, 1975: USNS *Eltanin* Southern Ocean oceanographic atlas. Contrib. No. 2256, Lamont-Doherty Geological Observatory.

Heinmiller, R. G., and R. G. Walden, 1973: Details of Woods Hole moorings. Woods Hole Oceanographic Institution, Tech. Rep. 73-71, 19 pp.

Joyce, T. M., and S. L. Patterson, 1977: Cyclonic ring formation at the polar front in the Drake Passage. *Nature*, **265**, 131–133.

Nowlin, W. D., Jr., T. Whitworth III and R. D. Pillsbury, 1977: Structure and transport of the Antarctic Circumpolar Current at Drake Passage from short-term measurements. *J. Phys. Oceanogr.*, **7**, 788–802.

Pillsbury, R. D., J. S. Bottero and R. E. Still, 1976: A compilation of observations from moored current meters. Vol. 9, *Currents, Temperature and Pressure in the Drake Passage during FDRAKE 75, January–March 1975*. School of Oceanography, Oregon State University, Data Rep. 65, Ref. 76-6.

——, —— and ——, 1977: A compilation of observations from moored current meters. Vol. 10, *Currents, Temperature and Pressure in the Drake Passage during FDRAKE 75, February 1975–February 1976*, School of Oceanography, Oregon State University, Data Rep. 67, Ref. 77-8.

Reid, J. L., and W. D. Nowlin, Jr., 1971: Transport of water through the Drake Passage. *Deep-Sea Res.*, **18**, 51–64.

Schwerdtfeger, W., 1962: Meteorologia del area del Pasaje Drake. Servicio Hidrogr. Nav., Argentina, H.410, 78 pp.

Sciremammano, F., R. D. Pillsbury, T. Whitworth, W. D. Nowlin, Jr., C. B. Fandry and D. J. Baker, 1978: Fluctuation scales for currents and temperatures from moored arrays in Drake Passage during 1975, 1976 and 1977. *Trans. Amer. Geophys. Union*, **59**, 810.

van Loon, H., 1967: The half-yearly oscillations in middle and high southern latitudes and the coreless winter. *J. Atmos. Sci.*, **24**, 472–486.